Cryorolling impacts on microstructure and mechanical properties of AISI 316 LN austenitic stainless steel

Yi Xiong, Yun Yue, Yan Lu, Tiantian He, Meixiang Fan, Fengzhang Ren, Wei Cao

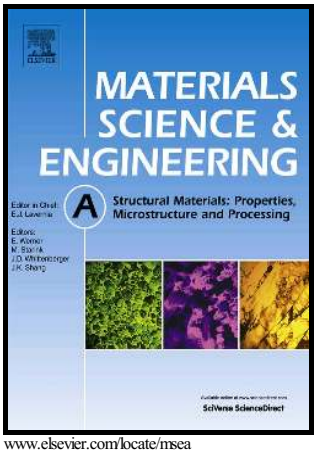

www.elsevier.com/locate/msea

PII: S0921-5093(17)31393-X
DOI: https://doi.org/10.1016/j.msea.2017.10.067
Reference: MSA35670

To appear in: *Materials Science & Engineering A*

Received date: 28 September 2017
Revised date: 19 October 2017
Accepted date: 20 October 2017

Cite this article as: Yi Xiong, Yun Yue, Yan Lu, Tiantian He, Meixiang Fan, Fengzhang Ren and Wei Cao, Cryorolling impacts on microstructure and mechanical properties of AISI 316 LN austenitic stainless steel, *Materials Science & Engineering A,* https://doi.org/10.1016/j.msea.2017.10.067

Cryorolling impacts on microstructure and mechanical properties of AISI 316 LN austenitic stainless steel

Yi Xiong [a,b], Yun Yue [c], Yan Lu [a], Tiantian He[c], Meixiang Fan[a], Fengzhang Ren [a,b], Wei CAO[d,e]

[a]School of Materials Science and Engineering, Henan University of Science and Technology, Luoyang 471023, China

[b]Collaborative Innovation Center of Nonferrous Metals, Luoyang 471023, China

[c]National United Engineering Laboratory for Advanced Bearing Tribology, Henan University of Science and Technology, Luoyang 471023, China

[d]Nano and Molecular Systems Research Unit, University of Oulu, FIN-90014, Finland

[e]School of Mechanical and Automotive Engineering, Anhui Polytechnic University, Wuhu 241000, China

*Corresponding author. Tel.: +86 379 64231269; fax: +86 379 64231943. E-mail address: xiongy@haust.edu.cn (Yi. Xiong).

Abstract

Microstructure evolution and mechanical properties of AISI 316 LN austenitic stainless steel (SS) after cryorolling with different strains were investigated by means of optical, scanning and transmission electron microscopy, X-ray diffractometer, microhardness tester, and tensile testing system. The deformation-induced martensite transition and the deformation microstructure occurred during cryorolling process were always composed of high-density dislocations, deformation twins, and deformation-induced martensites. Following the strain, the dislocation density in deformation microstructure approached saturation state and the volume fraction of deformation twins combined with deformation-induced martensites increased significantly. At the 70% strain, original austenite was transformed into martensite completely. Further increasing the strain to 90% would refine the martensitic lamellae to nanoscale. The deformation degree also led to remarkable increase of the strength and hardness of the cryorolled SS, and drastic reductions of the elongation. Due to the cryorolling, the tensile fracture morphology changed from typical ductile rupture to a mixture of quasi-cleavage and ductile fracture.

Keywords:

316 LN austenitic stainless steel; cryorolling; microstructure; mechanical properties; deformation-induced martensite transformation

1. Introduction

Austenitic stainless steel (SS) is one of the most attractive engineering alloys due to their good corrosion resistance and malleability [1]. However, a major drawback of austenitic steel is still in its low yield strength due to the presence of soft face centered cubic (fcc) γ-austenite phase [2, 3]. The strength can be improved by various treatments such as grain refinement, solid solution strengthening, and/or work-hardening. Among these methods, the work-hardening is more in favor for modern industrial production [4, 5] by utilizing the facile cold rolling process. However, during the rolling, dynamic recovery is prone to occur in the deformed microstructure, which reduces the strengthening effect. To circumvent these detrimental outcomes, the cryorolling, rolling under the circumstance of liquid nitrogen, is further developed.

Up to date, the cryorolling is mostly employed to prepare high-performance non-ferrous metals [6-10]. Only few studies involved ferrous metals. For example, Sabooni et al [11] investigated AISI 304L austenitic SS cold rolled at -15°C. The martensite morphology was changed from lath type to a mixture of lath and dislocation-cell types when the rolling reduction were higher than 60%. Kermanpur [12] has studied the volume fraction of deformation-induced martensite and mechanical properties of 316L austenitic SS subjected to heavy cold rolling at -15°C followed by annealing treatment. After 95% deformation, the amount of martensites was near 70% at low temperature and nano-grained (ranging from 30nm to 40nm) stainless steel can be obtained by short-time annealing at high temperature. Volume fraction of deformation-induced martensite and mechanical properties of 304L austenitic SS with different strain were also studied at a rolling temperature of -153°C [13]. The austenites were all transformed into martensites at strain above 80% and nano-grains were obtained. The mechanical properties were enhanced significantly. Cryorolling effect on microstructure and mechanical properties of 310S austenitic SS have been studied [14]. Although being lack of martensite transformation, heavy deformations during the cryorolling process produced nano-scaled grains and strengthened the investigated material. From the above works, it can be seen that the cryorolling technique has obvious advantages in enhancing the mechanical properties of the austenitic SS.

In this paper, the cryorolling treatment for the 316LN austenitic SS was conducted, and the structural evolution and mechanical properties during the treatment were analyzed. The 316 LN steel is selected due to its widely applications in petroleum, chemical industry, and nuclear power industries. However, apart from its outstanding intergranular corrosion and oxidation resistance, and excellent high-temperature mechanical properties, the low yield strength (only up to 200MPa after solid solution treatment) severely limited the application of 316LN austenitic SS in structural

material field. It is found that the cryorolling substantially enhanced the mechanical performances owing to the microstructural evolutions of the nano-sized grains during the rolling process. The deformation mechanism is also studied in details. It is hoped that this research will provide a reliable theoretical basis as well as technical support for the preparation of ultrafine grained austenitic SS and further expand its application field in steel industry.

2. Materials and methods

The 17.0 mm thick AISI 316LN stainless steel sheets in the present study were melted using a vacuum induction melting furnace (150 kg) followed by forging and hot rolling. The nominal composition (in wt. %) was listed as follows: 0.01C, 0.49Si, 0.87Mn, 17.09 Cr, 14.04 Ni, 2.56 Mo, 0.14 N and balance Fe. After solid solution treatment at 1050°C for 120min, single-phase austenitic microstructure with grain size about 80 μm was obtained (Fig. 1). Rectangular samples with size of 100×50×5 mm^3 were cut from the solid-solution sheet for the cryorolling process. All the samples were soaked in liquid nitrogen for 10 min. They were taken out quickly for multi-pass rolling operation using 5% reduction per pass to reach total reductions of 30%, 50%, 70%, and 90%, respectively. Immediately after the rolling pass, the samples were immersed in liquid nitrogen again for next pass.

Micro-tensile specimens were cut from the deformed materials to fit the required dimensions as illustrated in Fig. 2. Uniaxial tensile testing was carried out on an Instron 5980 mechanical test system and fracture surface morphology on a scanning electron microscope (SEM) at an accelerating voltage of 20kV. Microstructure characterization was performed via optical microscopy (OM, Zeiss Axio Vert A1) and transmission electron microscopy (TEM, JEOL-2100) operated at 200kV. X-ray diffraction (XRD) analysis was conducted to determine the phase composition of cryorolled austenitic SS using D8 ADVANCE X-ray diffractometer with Cu-Kα radiation. The scan angle was ranged from 35° to 100° with a step of 0.02°. The tube voltage and current were 40 kV and 40 mA, respectively. The volume fractions of deformation-induced martensite (Vα′) at different deformation degrees were calculated by using the (200), (220), (311) reflections of the austenitic phase (γ) and (200), (211), (220) reflections of the martensitic phase (α′) through the following formula:

$$V_{\alpha'}=\frac{1/n\sum_{j=1}^{n} I_{\alpha'}^{j}/R_{\alpha'}^{j}}{1/n\sum_{j=1}^{n} I_{\alpha'}^{j}/R_{\alpha'}^{j}+1/n\sum_{j=1}^{n} I_{\gamma}^{j}/R_{\gamma}^{j}}$$

Here n presents the number of selected reflections; I diffraction intensity factor; R scattering factor of materials. Three different sites were selected randomly to calculate $V_{\alpha'}$ and the mean value was considered as the volume fraction of deformation-induced martensite.

Microhardness was measured using MH-3 Vickers microhardness tester with 200g normal load, 10s loading time and 5s holding time on the polished region. An average microhardness value was determined based on five indentation measurements.

3. Results

3.1 Microstructure evolution

The XRD patterns of austenitic SS before and after cryorolling are depicted in Fig. 3. Obviously, the XRD of the cryorolled samples are different from that of single austenite after solid solution treatment. Even at the smallest deformation of 30%, diffraction peaks of α′ phases can be found. With the increasing strain, diffraction intensity of α′ martensite increased gradually and that of austenite decreased. Thus, the volume fraction of deformation-induced martensite increased, while the austenite decreased following the cryorolling process. As the deformation reached 70%, only martensite can be detected through the XRD pattern. All austenites were transformed into martensites. Meanwhile, diffraction peaks of martensite became wider with the deformation, especially at reductions of 70% and 90%. The broadening of diffraction peaks could be attributed to the interaction of large residual stress and grain refinement after cryorolling [15]. The similar broadening of diffraction peaks was also observed for cryorolled AISI 310S stainless steel [14].

The relationship curve between transformation of martensite and deformation is shown in Fig.4. A dramatic increase in the transformation of martensite follows the deformation degree. When the deformation is above 70%, original austenites are transformed into martensites completely (Fig. 3). As for 304L SS, the full transformation was achieved when true strain was 1.86 (about 80% in thickness reduction) during cryorolling at -153°C [13]. However, the result varies with rolling temperature. Kermanpur [16] found that the austenite could not be transformed to martensite completely even when the rolling deformation was up to 90% at room temperature. Similarly, the volume fraction of transformed martensite was only 18% when 316LN SS was compressed with a high strain of 60% at room temperature [17]. Based on the above evidences, the deformation-induced martensite transformation depends on the austenite stability (chemical composition and initial austenite grain size) and the rolling conditions (strain, stress state, strain rate, deformation temperature and rolling speed). The higher strain will lead to more defects in materials and easier nucleation of the martensite at defects [18]. The driving force for martensite transition is the free energy difference between the newly formed phases and the parent ones. The transition turns out when chemical driving force with addition of deformation-induced mechanical driving force reaches the one for a martensite transformation. Meanwhile, martensite transformation occurs by the nucleation and growth process. Considerably large free energy difference is produced when martensite transition takes place at a great super cooling temperature below the martensite starting temperature. This results in drastic decrease of the grain size

compared to that of stable growth. Furthermore, the dynamic recovery is significantly suppressed by the sudden drop of atomic diffusion at cryogenic temperature during rolling. Consequentially, abundant structure defects turn out in forms of dislocations. Due to the promoting effect of these defects on nucleation during phase transition, a large amount of deformation-induced martensites can be observed at the very early stage of cryorolling. The transformation rate and quantity could be remarkably improved by the introductions of low temperature and strain. At the present conditions, the austenites are fully transformed into martensites at strain of 70%.

Fig.5 shows the optical micrographs of cryorolled 316LN austenitic SS at different deformations. At the strain of 30%, the deformed microstructure is composed of a multiplicity of α′-martensites and slip lines as shown in Fig. 5a. Therein, slip lines are considered as the marks of dislocation gliding, by means of which the austenites can accommodate with the severe plastic strain during deformation. When the strain was increased to 50%, more slip lines appeared (Fig. 5(b)). Strong interactions can be also observed among the lines. The increase of the number of slip lines and the density, and the interactions between slip lines in different directions, provide more nucleation sites for deformation-induced martensites and also increase the amount of α′-martensite. At the 70% strain, deformation-induced martensites suffer from large plastic strains. They are elongated in the rolling direction and distributed in the form of long stripes (Fig. 5c). As the strain reached 90%, the strips were evolved to the fibers as shown in Fig. 5(d). This is own to the further intensified deformation degree of α′-martensites.

The TEM images after cryorolling are shown in Fig. 6. The deformation microstructure under a small strain is composed of high-density dislocations, deformation twins, and deformation-induced martensites (Fig 6a). With the increasing strain, dislocation density approaches its saturation and the quantity of deformation twins is also increased apparently. More deformation-induced martensites are formed due to the interactions between dislocations and deformation twins. Meanwhile, the martensite lath gradually becomes narrower. As shown in Fig. 6b-c, the width of martensite lath decreases from 200 nm (at strain of 30%) to 80 nm (at 70%). Further rolling after the saturation state can lead to breaking up of the lath-structured martensite resulting in smaller lathes and dislocation-cell type martensite [20–22]. Reportedly, the formation of slip bands during further rolling can be a reason of the change from lath to dislocation-cell type of martensite [23, 24]. As stated by Misra et al. [21], these two types of martensites are always presented simultaneously in the rolled samples after the saturation state, and further rolling only changes their volume fractions. With further increasing the strain to 90%, lamellar martensites are broken up evidently. A continuous diffraction ring appears in the following select-area electron diffraction (SAED) image, indicating the existence of the nano-grained martensites after cryorolling. The orientation of different grains is nearly of random distribution. Fig.6d also

identifies the martensitic grain size ranging from 30nm to 50nm.

3.2 Tensile properties and fractography

Fig. 7 shows the curve of ultimate tensile strength versus elongation of cryorolled 316LN austenitic SS at different strains. The strength index increases rapidly with the strain. The yield strength and ultimate tensile strength are increased from 209MPa and 527MPa (solid solution treatment) to 1468MPa and 1572MPa at 90% strain. However, the elongation decreases dramatically from 83% to 2%. At the beginning stage of deformation, the dramatic increase in strength is attributed to the increasing quantity of deformation-induced martensites and the enhanced hardening capacity. The latter serves a high growing rate in strength accompanied with a corresponding yield ratio ranging from 0.93 to 0.95. It is interesting that the yield ratio stays at ~0.93 after the full transformation of the austenites. However, the strength at 90% is obviously higher than that at 70%. The difference is mainly due to the refinement of martensite lath and nanocrystallization in microstructure. The microhardness distribution curve against strain is illustrated in Fig. 4. The development trend of hardness is very similar to that of strength. The original microhardness is 170HV for the solid-solution treated material. It increases from 415HV (at strain of 30%) to 528HV (at 90%) after imposing the strain. Compared with the original value, the microhadness can be improved 1.44 times (at 30%) and 2.1 times (at 90%) after the cryorolling.

Ren et al [25] stated that the main factors affecting the microhardness are dislocation density, grain size, and dislocation mobility. We investigated the mechanism that leads to the variations of the hardness in details. As stated above, the quantity of the deformation-induced martensites increases rapidly with the strain. They can anchor the dislocations effectively and hinder their motion as hard second phases. Meanwhile, a large amount of defects, including tangled dislocations generated during deformation, result in a dramatically increased dislocation density and high work hardening capacity. The other one is attributed to the refinement of martensite lath and nanocrystallization in microstructure. In one word, the rapid increase of microhardness is subjected to the increased dislocation density, impediment of dislocation motion, together with structure refinement or even nanocrystallization. Rolling metals and alloys at cryogenic temperatures suppresses dynamic recovery and recrystallization, leading to high dislocation density [26]. These high intensified structural defects could accelerate the nucleation as a part of martensite transition. A large amount of deformation-induced martensites appear at the initial stage of cryorolling. Thus, microhardness of the samples increases rapidly because of the work hardening and deformation-induced martensite transition. With further increase in the strain, the density of accumulated dislocations reaches its highest saturation level and the interactions of the dislocations are significantly enhanced, giving rise to the formation of large amounts of

deformation twins in the austenite structure. Much more nucleation sites for deformation-induced martensites are provided by the interactions between deformation twins as well as deformation twin and dislocation as shown in Fig. 8. The volume fraction of deformation-induced martensites become larger (Fig. 4). With the progressively increase of strain, the width of martensite lath become smaller. Meanwhile, the martensites are severely fragmented, denoted as the continuous ring in SAED. It is noticed that the similar SAEDs are typical for polycrystals dominated by large misorientation angles [27]. Thus, the present pattern clearly demonstrates the nano-scaled average grain size (<100 nm). Under the combined action of the aforementioned factors, the strength and hardness of investigated austenitic SS have a rapid increase but the elongation decline apparently.

The fracture morphology after tensile tests has been shown in Fig. 9. Before cryogenic rolling, solid-solution treated austenitic SS possesses excellent toughness and plasticity. Typical characteristics of ductile fracture are presented on the corresponding fracture surface. Small and shallow dimples (2−4 μm in size) surround large and deep ones with an average size of about 8μm. After cryorolling at 30% strain, the number of large and deep dimples decreases, but the small and shallow dimples increases. When the strain is 50%, both the number and the size of the large dimples reduce. Additionally, they are accompanied with vast cleavage facets, showing the mixed characteristic of quasi-cleavage and ductile fracture. As the strain is increased to 70%, the number and size continue to decrease whereas the area covered by cleavage facets increases. At 90% strain, the large and deep dimples have disappeared completely. Only a few of small dimples were kept at local regions. The fracture surface of cleavage facets owns the typical quasi-cleavage fracture characteristic.

4. Discussion

Based on the aforementioned microstructure characterizations of 316LN austenitic SS cryorolled at different strains, the microstructure evolution can be generalized as follows: (Ⅰ) high dense dislocations were generated and interacted with each other in original coarse-grain materials; (Ⅱ) deformation twins started to appeared when the dislocation density was close to a saturation state; (Ⅲ) the density of deformation twins increased and approached to the saturation condition; (Ⅳ) deformation-induced martensite transition occurs as a result of the interactions between dislocations, deformation twins, as well as dislocation and deformation twin; (Ⅴ) the austenite was transformed into martensite completely; (Ⅵ) the martensitic lath was refined; (Ⅶ) the refined martensite was fragmented further until nano-grained material was obtained.

As a typical metastable stainless steel with low stacking fault energy except for slip and twinning, martensite transition is another important deformation mode. In general, there are two kinds of transformation mechanisms from austenite to martensite as proposed by Sato [28] and Seetharaman [29]. (1) When the stacking fault energy of the base metal is below 18mJ/m^2, the

transformation of martensite follows the route of γ-austenite→ε-martensite→α′-martensite. (2) When the stacking fault energy of the base metal is above 18mJ/m^2, the path reads γ-austenite→ twin →α′-martensite. Previous researches [30, 31] showed that the stacking fault energy of 316LN austenitic SS was about 10 mJ/m^2. Thus, the transformation of martensite in 316LN austenitic SS follows the first path. However, the diffraction peak of ε-martensite was not found in the present XRD patterns (Fig. 3). This indicates that α′-martensite was mainly formed in 316LN austenitic SS after cryorolling. In this scenario, either the ε-martensite is too low to be detected, or it was eventually transformed to α′-martensite with more deformation.

The influences of the cryorolling on different steel types were compared. The 310S austenitic SS with stable state has the similar microstructure evolution under low deformation degree in the earlier research [14]. The dominating dislocation slip lines were formed with a small amount of deformation twins at the same time. Differences mainly stay with the occurrence of deformation-induced martensite transitions. For both steels, the dislocation density reached the saturation state with the increase of strain. Dramatic increases were found for the quantity of deformation twins, and their interactions. While abundant twin-matrix lamellae appear in AISI 310S austenitic SS matrix, nucleation sites of martensite were increased in 316LN austenitic SS as shown in Fig. 9. These nucleations lead to larger volume fraction of the martensite until the full transformation of the austenitic microstructure to the martensitic counterpart. After the strain was increased to 90%, dislocation arrays and twin–twin intersections further subdivided the twin–matrix lamellae into nanometer-sized blocks for the AISI 310S austenitic SS. This is in good accordance with the refinement mechanisms of the 304 austenitic SS subjected to laser shock [32] and the nano-grained metallic materials with low stacking fault energies during surface mechanical attrition treatment [33]. Whereas, the lath martensite in 316LN austenitic SS is further refined and broken, which leads to the formation of the nanometer martensite grains. XRD patterns show that the austenite has been transformed into martensite completely at cryorolling strain of 70%. If the increased strain exceeded 70%, it must be the deformation-induced martensites which endured the severe deformation. As aforementioned above, the deformation-induced martensite can be divided into lamellar martensite and dislocation-cell martensite. It was not surprising that the lath martensite would turn into dislocation-cell martensite at last along with the increase of strain.

The deformation microstructures of low-carbon martensitic steel subjected to cold rolling were categorized into three kinds of morphologies by Tsuji [34] including ultrafine lamella dislocation cell (LDC), irregularly bent lath (IBL), and kinked lath (KL). In the present study, the deformation microstructure was mainly composed of LDCs because of the much higher strain than that in Reference [34]. Meanwhile, the cryogenic temperature when rolling suppressed the

dynamic recovery of dislocations and other substructures, which resulted in a further increase of the density of substructures such as dislocations and deformation twins et al. Dislocation walls formed due to high-density dislocation tangling accompanied with deformation twins further subdivided the LDCs and the martensitic microstructure was refined to nanometer scale eventually. Ye et al [35] have prepared the gradient nanostructured 304 SS with high strength and toughness by means of Ultrasonic Nano-crystal Surface Modification. The corresponding nanocrystallization mechanism was considered to be the cooperation of deformation-induced martensite and deformation twin, which was in good accordance with the refinement mechanism in this investigation.

5. Conclusions

The effect of cryorolling on the microstructure and mechanical properties of AISI 316 LN austenitic SS has been investigated systematically. The conclusions can be drawn as follows：

1. During cryorolling and the volume fraction of transformed martensite, deformation-induced martensite transition occurs in 316LN austenitic SS increases rapidly with the increasing strain. Deformation microstructures are all composed of high density dislocations, deformation twins, and deformation-induced martensites, but the contribution of the three components varies obviously at different strains. As strain is increased to 70%, the original austenites are transformed to martensites completely. Further increasing the strain to 90%, transformed martensitic lamellae is refined to nanoscale.

2. The strength and microhardness of 316 LN austenitic SS increases significantly with the increasing cryorolling deformation. When the strain reaches 90%, the yield strength, ultimate tensile strength, and microhardness increase from 209MPa, 527MPa and 170HV (no deformation) to 1468MPa, 1572MPa and 528HV, respectively. However, the elongation decreases from 83% to 2%. The corresponding tensile fracture morphology changes from typical ductile rupture to a mixture of quasi-cleavage and ductile fracture.

3. Ending up with nano-grained material, the 316LN austenitic SS during cryorolling have endured the evolution process in the order of the generation and interaction of high dense dislocations, deformation twins, deformation-induced martensite transition, and the refinement even fragmentation of martensite.

Acknowledgements

This work was supported by the National Natural Science Foundation of China under grants Nos. 50801021 and 51201061, and by the Program for Science, Technology Innovation Talents in Universities of Henan Province (17HASTIT026), the Science and Technology Project of Henan Province (152102210077), Education Department of Henan Province (16A430005) and the

Science and Technology Innovation Team of Henan University of Science and Technology (2015XTD006).

References

[1] S. D. Washko, and G. Aggen, ASM handbook vol 1: properties andselection, 3rd ed, ASM International, New York (2005), 1303.

[2] L. P. Karjalainen, T. Taulavuori, M. Sellman, A. Kyröläinen. Some strengthening methods for austenitic stainless steels. Steel Research International, 2008, 79: 404-412.

[3] I. Shakhova, V. Dudko, A. Belyakov, K. Tsuzaki, R.Kaibyshev. Effect of large strain cold rolling and subsequent annealing on microstructure and mechanical properties of an austenitic stainless steel. Materials Science & Engineering A, 2012, 545:176-186

[4] J. X. Huang, X. N. Ye, Z. Xu. Effect of cold rolling on microstructure and mechanical properties of AISI 301LN metastable austenitic stainless steels. Journal of Iron and Steel Reaearch, International. 2012, 19(10): 59-63.

[5] T. Morikawa , K. Higashida. The role of deformation twinning in the formation of a fine-grained structure in cold-rolled 310 steel. Journal of Materials Science, 2006, 41 : 2581-2585

[6] Y.M. Wang, M.W. Chen, F.H. Zhou, E. Ma, High tensile ductility in a nanostructured metal. Nature,2002, 419: 912-917

[7] S.V. Zherebtsov, G.S. Dyakonov, A.A. Salem, V.I. Sokolenko, G.A. Salishchev, S.L. Semiatin.Formation of nanostructures in commercial-purity titanium via cryorolling. Acta Materialia, 2013,61(4): 1167-1178

[8] S. K.Panigrahi, R. Jayaganthan. Development of ultrafine grained high strength age hardenable Al 7075 alloy by cryorolling. Materials and Design, 2011, 32 :3150-3160

[9] D.F.Guo , M.Li , Y.D.Shi , Z.B.Zhang , T.Y.Ma , H.T.Zhang , X.Y.Zhang. Simultaneously enhancing the ductility and strength of cryorolled Zr via tailoring dislocation configurations. Materials Science & Engineering A, 2012, 558: 611-615

[10] J. Das. Evolution of nanostructure in α-brass upon cryorolling. Materials Science & Engineering A, 2011, 530:675-679

[11] S. Sabooni , F. Karimzadeh , M.H. Enayati , A.H.W. Ngan.The role of martensitic transformation on bimodal grain structurein ultrafine grained AISI 304L stainless steel. Materials Science & Engineering A, 2015, 636:221-230

[12]M. Eskandari, A. Najafizadeh, A. Kermanpur .Effect of strain-induced martensite on the formation of nanocrystalline 316L stainless steel after cold rolling and annealing. Materials Science & Engineering A, 2009, 519: 46-50

[13] B. Roy, R. Kumar ,J. Das. Effect of cryorolling on the microstructure and tensile properties of

bulk nano-austenitic stainless steel. Materials Science & Engineering A, 2015, 631 :241-247

[14] Y. Xiong, T.T. He, J.B. Wang, Y. Lu , L.F. Chen, F.Z. Ren ,Y.L. Liu , Alex A. Volinsky. Cryorolling effect on microstructure and mechanical properties of Fe–25Cr–20Ni austenitic stainless steel. Materials and Design, 2015, 88: 398-405

[15] G. Sunkulp, K. Nachiket, R. Jayaganthan, I.V. Singh, D. Srivastava, G.K. Dey, N. Saibaba, Mechanicalbehaviour and microstructural characterizations of ultrafine grained Zircaloy-2 processed by cryorolling. Materials Science & Engineering A, 2014, 603: 23-29.

[16] A. Hedayati, A. Najafizadeh, A. Kermanpur , F. Forouzan. The effect of cold rolling regime on microstructure and mechanical properties of AISI 304L stainless steel.Journal of Materials Processing Technology, 2010, 210: 1017-1022.

[17] J. Manjanna, S. Kobayashi, Y. Kamada, S. Takahashi, H. Kikuchi. Martensitic transformation in SUS 316LN austenitic stainless steel at RT. Journal of Materials Science, 2008, 43:2659-2665

[18] S. G. Chowdhury, S. Das, P.K. De. Cold rolling behaviour and textural evolution in AISI 316L austenitic stainless steel. Acta Materialia, 2005, 53: 3951-3959.

[19] T. Shintani, Y. Murata. Evaluation of the dislocation density and dislocation character in cold rolled type 304 steel determined by profile analysis of X-ray diffraction. Acta Materialia, 2011; 59: 4314-4322

[20] R.D.K. Misra, V.S.A. Challa, P.K.C. Venkatsurya, Y.F. Shen, M.C. Somani, L.P. Karjalainen. Interplay between grain structure, deformation mechanisms and austenite stability in phase-reversion-induced nanograined/ultrafine-grained austenitic ferrous alloy. Acta Materialia, 2015, 84: 39-348.

[21] R.D.K. Misra, J.S. Shah, S. Mali, P.K.C. Venkata Surya, M.C. Somani, L.P. Karjalainen, Phase reversion induced nanograined austenitic stainless steels: microstructure, reversion and deformation mechanisms . Materials Science and Technology , 2013, 29 (10): 1185-1192.

[22] S. Rajasekhara, L.P. Karjalainen, A. Kyröläinen, P.J. Ferreira, Microstructure evolution in nano/submicron grained AISI 301LN stainless steel . Materials Science & Engineering A,2010,527: 1986-1996.

[23] S. Takaki, K. Tomimura, S. Ueda, Effect of pre-cold-working on diffusional reversion of deformation induced martensite in metastable austenitic stainless steel . ISIJ International, 1994,34 (6):522-527.

[24] K. Tominiura, Y. Kawauchi, S. Takaki, Y. Tokunaga, Effect of prior deformation on grain refining process of martensitic shear reversion in metastable austenitic stainless steel. Journal of the Iron and Steel Institute of Japan, 1991, 77 (9): 1519-1526.

[25] F.Z. Ren, S.Y. Zhao, W.H. Li, B.H. Tian, L.T. Yin, A.A. Volinsky, Theoretical explanation of Ag/Cu and Cu/Ni nanoscale multilayers softening. Materials Letters, 2011,65: 119-121

[26] D. Singh, P.N. Rao, R. Jayaganthan, Effect of deformation temperature on mechanical properties of UFG Al–Mg alloys processed by rolling.Materials and Design, 2013, 50(17) :646-655.

[27] H. Ueno, K. Kakihata, Y. Kaneko, S. Hashimoto, A. Vinogradov, Enhanced fatigue properties of nanostructured austenitic SUS 316L stainless steel. Acta Materialia, 2011, 59: 7060-7069.

[28] A.Sato, K. Soma, T.Mori, Hardening due to pre-existing ε-Martensite in an Fe-30Mn-1Si alloy single crystal, Acta Metallurgica, 1982, 30:1901-1907

[29] V.Seetharaman, R. Krishnan, Influence of the martensitic transformation on the deformation behaviour of an AISI 316 stainless steel at low temperatures, Journal of Materials Science, 1981, 16(2): 523-530

[30] T.S. Byun, N. Hashimoto, K. Farrell. Temperature dependence of strain hardening and plastic instability behaviors in austenitic stainless steels. Acta Materialia, 2004, 52: 3889-3899.

[31] T.S. Byun, E.H. Lee, J.D. Hunn, Plastic deformation in 316LN stainless steel-characterization of deformation microstructures, Journal of Nuclear Materials, 2003, 321:29-39

[32] J.Z. Lu , K.Y. Luo , Y.K. Zhang, G.F. Sun , Y.Y. Gu , J.Z. Zhou , X.D. Ren ,X.C. Zhang , L.F. Zhang , K.M. Chen , C.Y. Cui , Y.F. Jiang , A.X. Feng , L. Zhang. Grain refinement mechanism of multiple laser shock processing impacts on ANSI 304 stainless steel.Acta Materialia, 2010, 58 : 5354-5362

[33] H. W. Huang, Z. B. Wang, J. Lu, K. Lu. Fatigue behaviors of AISI 316L stainless steel with a gradient nanostructured surface layer. Acta Materialia, 2015, 87: 150-160.

[34] R. Ueji , N. Tsuji, Y. Minamino, Y. Koizumi. Ultragrain refinement of plain low carbon steel by cold-rolling and annealing of martensite. Acta Materialia, 2002, 50: 4177-4189

[35] C. Ye, A. Telang, A.S. Gill , S. Suslov , Y. Idell, K. Zweiacker, JörgM.K. Wiezorek , Z. Zhou , D. Qian, S.R. Mannava, V.K. Vasudevan. Gradient nanostructure and residual stresses induced by Ultrasonic Nano-crystal Surface Modification in 304 austenitic stainless steel for high strength and high ductility. Materials Science & Engineering A, 2014, 613:274-288

Figures:

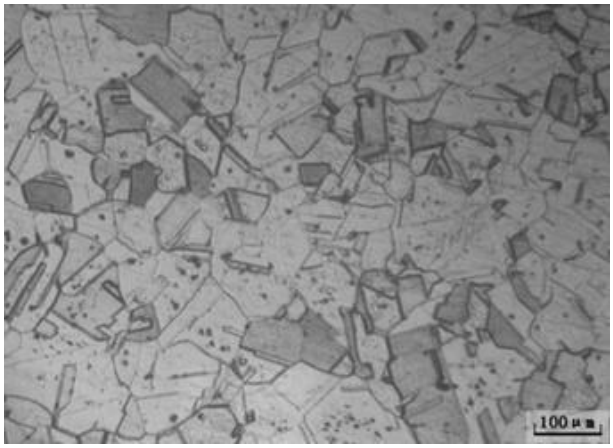

Fig. 1. Microstructure of 316LN stainless steel after solution treatment.

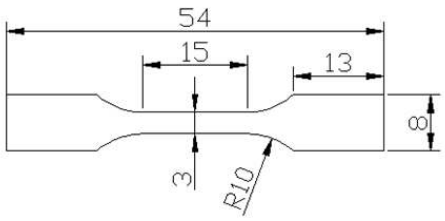

Fig. 2. The dimension of tensile sample.

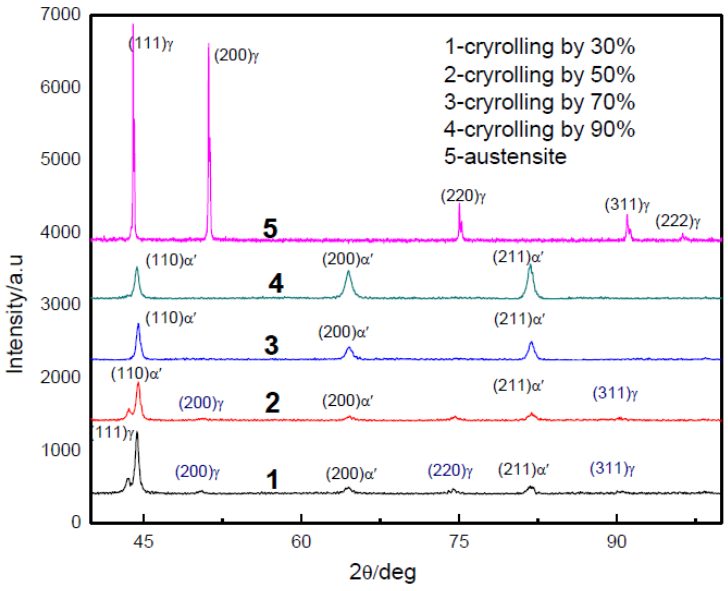

Fig. 3. XRD patterns of the 316LN austenitic stainless steel before and after cryorolling.

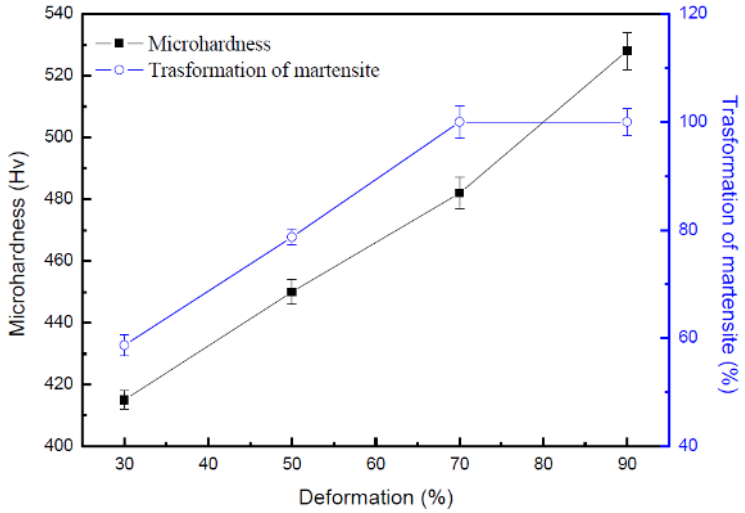

Fig. 4. The relationship between the volume fraction of the martensite, microhardness and the cryorolling deformation.

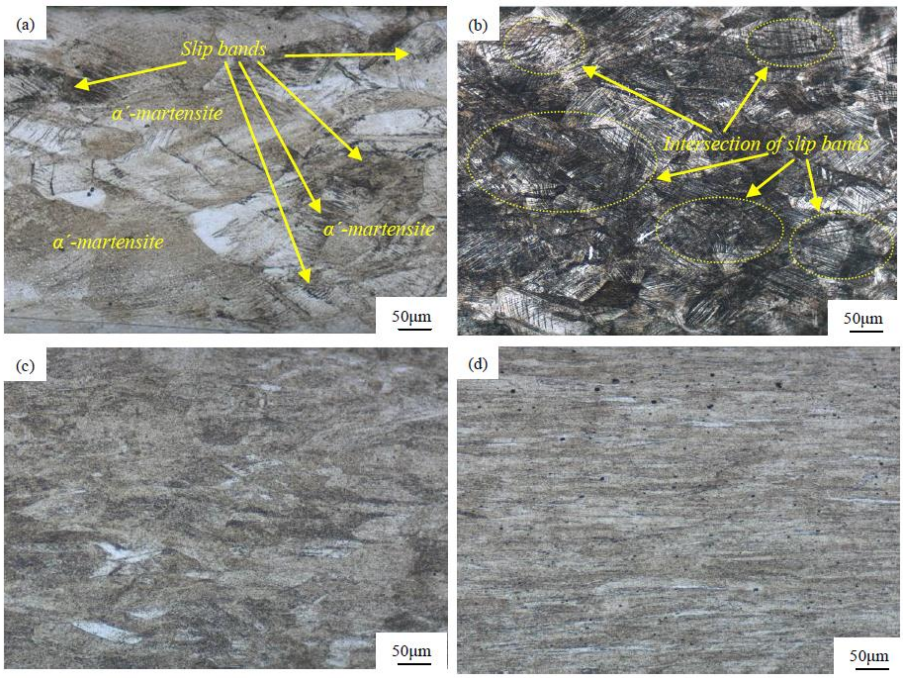

Fig. 5. Metallographic structure of the 316LN austenitic stainless steel after cryorolling: (a) after 30% deformation; (b) after 50% deformation; (c) after 70% deformation; (d) after 90% deformation.

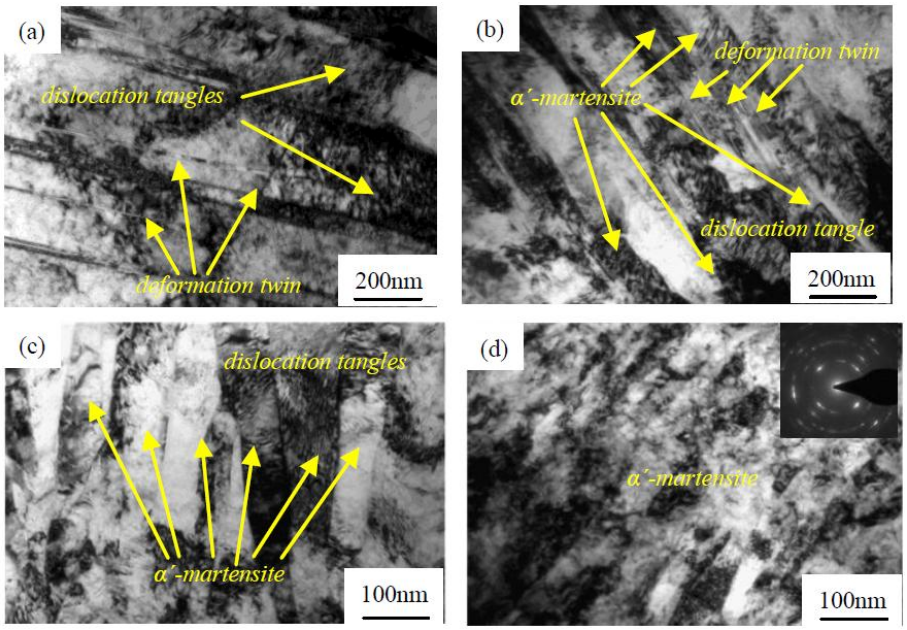

Fig. 6. TEM images of the 316LN austenitic stainless steel after cryorolling: (a) after 30% deformation; (b) after 50% deformation; (c) after 70% deformation; (d) after 90% deformation.

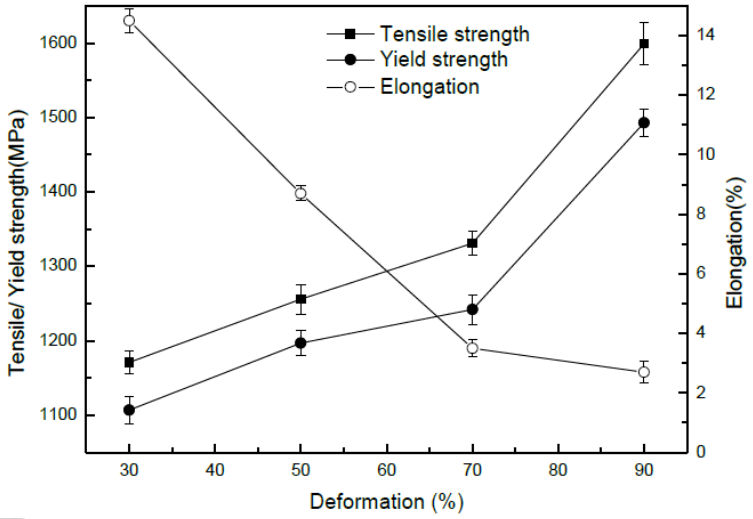

Fig. 7. Mechanical properties of the 316LN austenitic stainless steels after cryorolling.

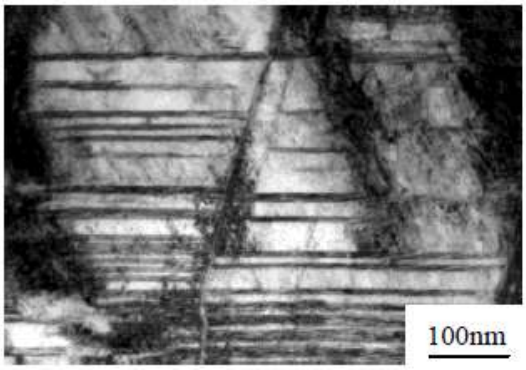

Fig. 8. Interaction of the deformation twins.

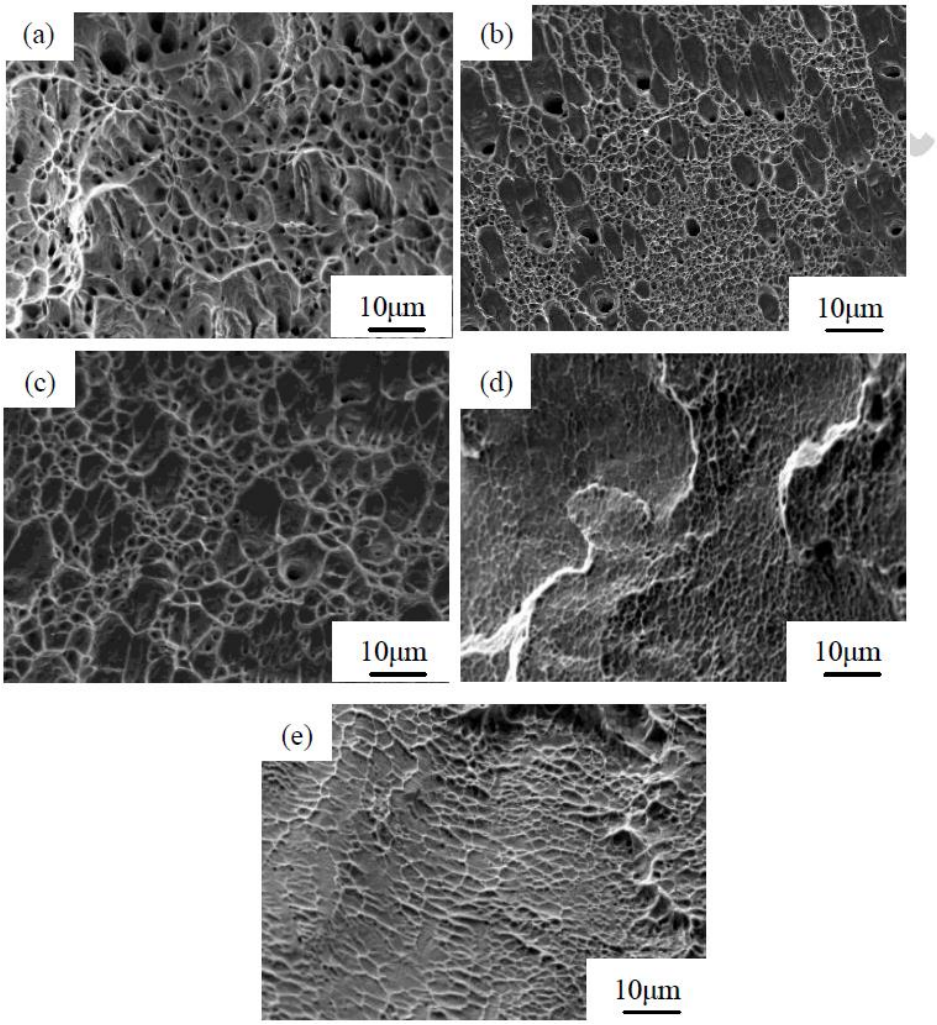

Fig. 9. Fracture surface morphology of the 316LN austenitic stainless steel before and after cryorolling: (a) original austenite structure; (b) after 30% deformation; (c) after 50% deformation; (d) after 70% deformation; (e) after 90% deformation.